Suspensions of Colloidal Plates in a Nematic Liquid Crystal: A Small Angle X-ray Scattering Study

Claire Pizzey[1], Susanne Klein, Edward Leach, Jeroen S. van Duijneveldt[1], Robert M. Richardson[2]
Hardcopy Technology Laboratory
HP Laboratories Bristol
HPL-2003-270
January 8th , 2004*

Suspensions of anisometric particles in the nematic phase of a liquid crystalline host solvent were prepared. We chose Claytone AF, a commercial quaternary ammonium surfactant treated montmorillonite, with an aspect ratio of up to 1:2000, and dimethyldioctadecylammonium bromide treated Laponite, with an aspect ratio of 1:8 as the dispersed particles. K15, a nematogenic compound (also known as 5CB), was the dispersing medium. The suspensions were characterised by small angle X-ray scattering (SAXS). The liquid crystal delaminates the clays well, but the scattering curves from Claytone suspensions have prominent first and second order pseudo Bragg peaks, indicating that stacking of clay plates has occurred. We report a model for fitting SAXS data based on Hosemann's theory for suspensions of plane parallel sheets.

* Internal Accession Date Only Approved for External Publication
[1] School of Chemistry, Cantock's Close, University of Bristol, Bristol, BS8 1TS
[2] H.H. Wills Physics Laboratory, Tyndall Avenue, University of Bristol, Bristol, BS8 1TL

Suspensions of Colloidal Plates in a Nematic Liquid Crystal: A Small Angle X-ray Scattering Study

Claire Pizzey*, Susanne Klein[+], Edward Leach[+], Jeroen S. van Duijneveldt* and Robert M. Richardson[#]

*** School of Chemistry, Cantock's Close, University of Bristol, Bristol, BS8 1TS.**
[+] HP Laboratories, Filton Road, Stoke Gifford, Bristol, BS34 8QZ.
[#] H.H. Wills Physics Laboratory, Tyndall Avenue, University of Bristol, Bristol BS8 1TL.

Abstract

Suspensions of anisometric particles in the nematic phase of a liquid crystalline host solvent were prepared. We chose Claytone AF, a commercial quaternary ammonium surfactant treated montmorillonite, with an aspect ratio of up to 1:2000, and dimethyldioctadecylammonium bromide treated Laponite, with an aspect ratio of 1:8 as the dispersed particles. K15, a nematogenic compound (also known as 5CB), was the dispersing medium. The suspensions were characterised by small angle X-ray scattering (SAXS). The liquid crystal delaminates the clays well, but the scattering curves from Claytone suspensions have prominent first and second order pseudo Bragg peaks, indicating that stacking of clay plates has occurred. We report a model for fitting SAXS data based on Hosemann's theory for suspensions of plane parallel sheets.

Introduction

Most reported liquid crystal colloids involve the suspension of spherical particles, such as colloidal silica or polymer lattices, in a liquid crystalline host. [Stark 2001] Spheres, treated with a polymeric stabiliser, cause the formation of topological defects and disruption of the nematic matrix. The matrix acts to expel the spheres to minimise the energy in the system and a defect stabilised network structure, called a "filled nematic", results [Kreuzer and Eidenschink 1996]. We are interested in suspensions that do not flocculate when cooled from the isotropic into the nematic phase, i.e. where the particles are not expelled. Plates cause fewer topological defects and with careful tuning, a good dispersion that minimises the potential for defect structures may be prepared [Kawasumi *et al* 1999, 1996]. These systems could exhibit interesting ordering and phase behaviour as compared to the pure host material. It is therefore crucial to characterise the interaction of the dispersed particles with the dispersing medium. The maximum dimensions of the plates are approximately 2 μm for Claytone and much less (0.03 μm) for Laponite. These are too small to lead to conclusive results when the suspensions are inspected under a polarisation microscope. Light scattering is not suitable when the liquid crystal is in the nematic phase as the signal generated by nematic domains cannot be easily differentiated from the signal generated by the dispersed particles. Small angle X-ray scattering (SAXS) is the preferred characterisation method. The apparatus we have used has a scattering vector-range from 0.03 $Å^{-1}$ to 0.6 $Å^{-1}$ so we can probe a size range between 10 Å and 200 Å. Although this does not allow determination of the diameter of suspended

Claytone or even Laponite particles, we are able to see whether the clays delaminate completely or form periodic structures.

Sample preparation

In order to limit the defect formation a low molecular weight surfactant, rather than a polymeric surface treatment, was chosen to stabilise the particles in the suspension against mutual attractive forces and subsequent aggregation.

The two types of clay plates used are of similar chemical structure but differ greatly in aspect ratio. Claytone AF (Southern Clay Products) is a surface treated natural montmorillonite clay with a thickness of approximately 1nm and a range of diameters from 500nm to 2000nm [van Olphen 1977] (see Figure 1). With this high aspect ratio the particles are not rigid plates but have some flexibility as can be seen in the micrograph. Claytone is commercially pre-treated with dihydrogenated tallow, a surfactant mixture, the main component of which is dimethyldioctadecylmmonium bromide (DODAB) [Ho 2001] to give stable suspensions in non-aqueous solvents. The treated clay was cleaned repeatedly with a 40/60 mixture of propanol and water (ultra pure, Millipore) to remove excess surfactant, dried under vacuum and finely ground prior to use.

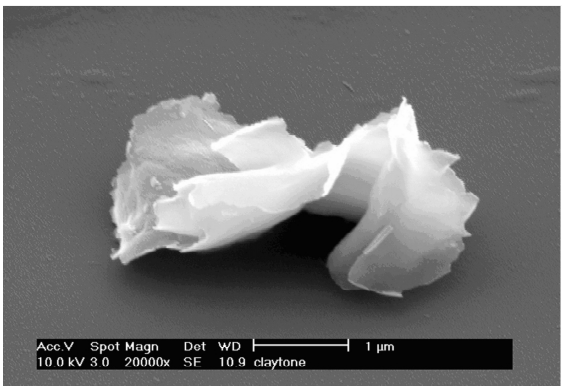

Figure 1: Electron micrograph of Claytone AF. The image shows clearly that the plates are rather flexible structures.

Laponite RD (Rockwood Additives) is a synthetic hectorite type clay with a thickness of approximately 1nm and a diameter of 25nm [Rockwood Additives 2003]. Laponite was totally dispersed in water (1 g, 1% w.w.) by stirring for 24 hours prior to surfactant treatment. The surfactant DODAB (Acros Chemicals, used as received) was added in dilute solution in an 80:20 water:propanol mix to give 100% coverage using the Cation Exchange Capacity (CEC) calculated in reference [Cione *et al* 1998]. The treated clay was cleaned by repeated washing and was subsequently dried under vacuum to remove all traces of water. [Jordan 1949] The particles were finely ground with an agate pestle and mortar and dried prior to suspension in the isotropic phase of the liquid crystal. Inspection by scanning electron microscopy (SEM) shows that Laponite when delaminated consists of plates with diameters smaller than 100nm (see Figure 2).

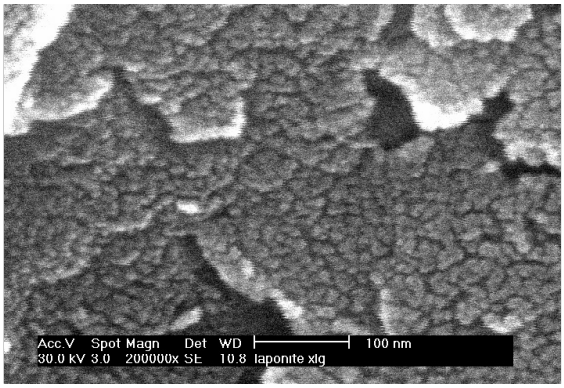

Figure 2: Electron micrograph of Laponite. The image shows aggregates and smaller structures which could be single particles since their maximum dimension is smaller than 50nm.

Laponite has a strong tendency to form films when suspended in water and then dried on a clean piece of glass. To get a glimpse of single plates under the SEM we used very dilute suspensions (1 part of Laponite in 1000 parts of water) and sprayed these suspension on a heated glass slide (180 °C) to avoid droplet formation and hence agglomeration of the Laponite particles. Even after this treatment single particles could only be seen in between agglomerates. These single particles have a diameter, *d*, of less than 100 nm confirming the literature values of 10nm < *d* < 40nm [Balnois et al 2003] and 20nm < *d* < 95nm [Zhivkov and Stoylov 2002].

The liquid crystal chosen was K15 (4-pentyl-4'-cyanobiphenyl, Merck, used as received) due to its high purity and room temperature nematic phase. K15 is a widely used liquid crystal with a nematic – isotropic transition temperature (T_{NI}) of 35°C [BDH 1986]. It is well known that this transition temperature is easily shifted by trace impurities. Adding clean, dry stabilised clay does not shift T_{NI} (although we have previously observed a decrease of T_{NI} for solvent contaminated samples) and therefore we conclude that the stabiliser is irreversibly attached to the plates and does not dissolve into the liquid crystal. The particles do not behave as chemical contaminants. A shift in T_{NI} in the suspensions would therefore be indicative of contamination in the sample.

The clay suspensions were prepared by adding the dry powder to the isotropic phase of the liquid crystal and stirring for 15 minutes. This was followed by 6-7 hours of sonication, degassing under vacuum and then cooling to the nematic phase. The particles did not sediment and the suspension was then stable for up to 24 hours, after which time flocculation was observed. The sample then developed two discrete layers, one particle poor and the other particle rich with an open floc structure. The aggregates were easily broken up, 15 minutes of stirring at approximately 40°C restored a good suspension.

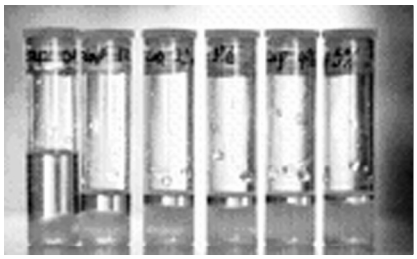

Figure 3: Phase separation after 40 hours. From left to right: 0.5wt% , 1wt%, 2wt%, 3wt%, 4wt% and 5 wt% of DODAB stabilised Laponite in K15.

Small Angle X-ray Scattering

SAXS measurements over a temperature range from 25°C to 40°C were performed at the University of Bristol Physics Department. The diffraction measurements were made using copper Kα X-rays (averaged λ = 0.154 nm), from a sealed tube with other wavelengths removed using a nickel filter and a graphite monochromator. The diffraction pattern was detected using a multi-wire area detector [Bateman *et al* 1987]. It was placed at 840 mm from the sample with an evacuated path so that a Q (scattering vector) range from 0.03 $Å^{-1}$ to 0.6 $Å^{-1}$ was covered. The sample to detector distance was calibrated using a silver behenate standard [Huang *et al* 1993]. The suspensions were filled into Lindemann glass capillaries (diameter 2mm, wall thickness 0.01mm) which had been flattened to give a path length of ~1mm for the X-ray beam. The samples were cooled from the isotropic phase in an ~0.5T magnetic field.

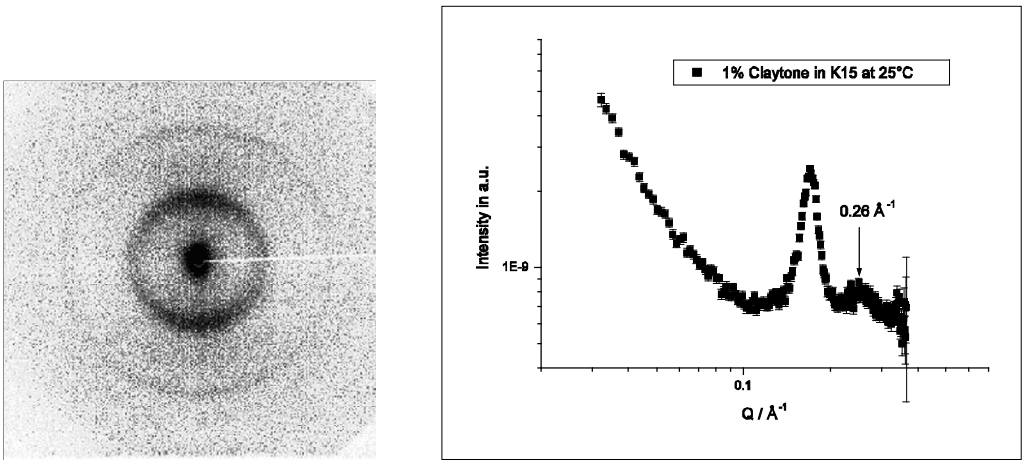

a b

Figure 4. Scattering from 1% Claytone in K15 at 25°C with vertical director in the form of (a) detector image and (b) the azimuthally averaged scattering from a vertical band as a function of the scattering vector, Q. No detector efficiency or background correction has been applied. The peak corresponding to 0.26 $Å^{-1}$ is due to K15. The other two peaks are respectively first and second order pseudo Bragg peaks from the suspended particles.

The measured counts were corrected for the efficiency of each pixel by dividing the data by the counts from a ^{55}Fe radioactive source, which gave an isotropic flood of X-rays. The transmission of the samples was determined during the data acquisition runs by taking the counts from the main beam (after passing through an attenuating beam stop) on the detector. The transmission was determined as the ratio of these counts with and without the sample in the beam.
The scattering from the liquid or liquid crystal host was subtracted from the scattering from the dispersions using the formula,

$$I_{correct} = \frac{I_{L+P}}{T_{L+P}R_{L+P}} - \frac{I_L}{T_L R_L} \qquad (1)$$

where I_{L+P} is the intensity from the dispersion (Liquid +Particles) in a sample tube, T_{L+P} is the transmission of the dispersion in a sample tube and R_{L+P} is the length of

the run. I_L, T_L and R_L are the corresponding quantities for a sample of the pure dispersion medium (Liquid only). Since the dispersion only contains a few percent of clay and the sample tubes were nominally the same thickness, this formula gives a reasonable correction for the scattering from the liquid host and the container. After the background correction, the data was azimuthally averaged in order to improve statistics and make the scattering from the isotropic and nematic phases comparable.

Theoretical background

This section outlines the background theory for the scattering from suspensions of plate-like objects. In particular, we consider how the proportion of plates that are stacked and the characteristics of the stacks influence the scattering.

We have assumed that the particles are either single plates of clay or stacks of plates with some intervening surfactant and/or host. For sufficiently dilute suspensions (typically <1% by volume) inter-particle interference may be neglected. The scattering from an anisotropic particle may be calculated from the square of the single particle structure factor, averaged over all orientations of the particle with respect to the scattering vector, **Q**. For simplicity we will consider disc-shaped plates although it turns out that, in the Q range of interest, the scattering is insensitive to the in-plane shape of the plates. The structure factor of a particle with cylindrical symmetry is given as the product of a radial and an axial structure factor.

$$F(\mathbf{Q}) = F_a(Q\cos\theta).F_r(Q\sin\theta) \quad (2)$$

where θ is the angle between the cylindrical axis and the scattering vector, **Q**. The scattering from an assembly of perfectly aligned identical particles depends on the number of particles illuminated by the incident beam, the electron density contrast between a particle and the solvent, $\Delta\rho$, and the square of the structure factor:

$$I(\mathbf{Q}) = N_P\ \Delta\rho^2\ F_a^2(Q\cos\theta)\ F_r^2(Q\cos\theta). \quad (3)$$

For samples where the cylindrical axis may point in any direction at random the scattering depends on the orientational average of the structure factor.

$$I(Q) = N_P \Delta\rho^2 \int_0^{\pi/2} F_a^2(Q\cos\theta) F_r^2(Q\cos\theta)\sin\theta d\theta \quad (4)$$

For discs, the radial structure factor is given by an expression containing the first order Bessel function, J_1,

$$F_r(Q\sin\theta) = \pi r^2 \frac{2J_1(Qr\sin\theta)}{Qr\sin\theta} \quad (5)$$

where *r* is the radius. At low Q, this expression tends to πr^2, the cross-sectional area of the disc. For single discs, the axial structure factor is given by the expression,

$$F_a(Q\cos\theta) = h\frac{\sin(Q(h/2)\cos\theta)}{Q(h/2)\cos\theta} \quad (6)$$

where *h* is the thickness of the disc. At low *Q*, this expression tends to *h*, the thickness of the disc. For isolated discs, the scattering can be calculated by performing the average in equation 4 numerically [Lin et al 1987]. However, in this work, the pseudo Bragg peaks in the data suggested that the discs were stacked to some extent. We therefore consider possible models for the stacking.

Initially we considered the most general model available for the stacking of the discs. For stacks of discs, the structure factor depends on the number of discs in a stack, *M*,

the disc or "hard" phase thickness, *h*, and the gap or "soft" solvent phase thickness, *s*. In addition, there may be some variation in the thickness of the "hard" phase and the "soft" phase. We assumed that these variations have gaussian distributions characterized by the standard deviations, σ_h and σ_s. In this case, the axial structure factor may be calculated using the expressions given by Hosemann [Hosemann and Bagchi 1962]:

$$F_a(Q\cos\theta) = I_B(Q\cos\theta) + I_C(Q\cos\theta) \qquad (7)$$

The first term, known as the "Babinet" term, produces pseudo Bragg peaks at *Q* values corresponding to $2\pi/(h+s)$ and tends to zero at zero *Q*. The second term, known as the "crystal" term, is the coherent scattering from the whole stack and tends to $(Mh)^2$ at low *Q*. These two terms are given by the expressions:

$$I_B(Q\cos\theta) = \frac{2M}{Q^2}\,\mathrm{Re}\left(\frac{(1-F_h)(1-F_s)}{1-F_hF_s}\right)$$

$$I_C(Q\cos\theta) = \frac{2}{Q^2}\,\mathrm{Re}\left\{F_s\left(\frac{1-F_h}{1-F_sF_h}\right)^2\left[1-(F_sF_h)^M\right]\right\}, \qquad (8)$$

where F_h and F_s are the Fourier transforms of the distributions of "hard" and "soft" phase thicknesses and for gaussian distributions they are given by the expressions,

$$F_h(Q) = \exp(-iQh)\exp\left(-\frac{Q^2\sigma_h^2}{2}\right)$$

$$F_s(Q) = \exp(-iQs)\exp\left(-\frac{Q^2\sigma_s^2}{2}\right). \qquad (9)$$

The final expression for the scattered intensity for a collection of stacks of *M* discs becomes:

$$I_M(Q) = N_P\Delta\rho^2V_D^2\int_0^{\pi/2}\left(\frac{2J_1(Qr\sin\theta)}{Qr\sin\theta}\right)^2\left(\frac{I_B(Q\cos\theta)+I_C(Q\cos\theta)}{h^2}\right)\sin\theta\,d\theta \qquad (10)$$

where the volume of a single disc, V_D, has been factorised out. The integral may be evaluated numerically and the effect of polydispersity of the disc radius and the number of discs in a stack may be included by numerical averaging over a gaussian distribution of *r* and *M*. However, for $Q \geq \pi/r$ the Bessel function only contributes to the integral for $Qr\sin\theta \sim 0$ and the integration over θ introduces a factor of $2\pi/(AQ^2)$ where *A* is the area of the disc [Kratky and Porod 1948]. Since Q(min)~0.03Å^{-1} and $r \geq 100$ Å, all the data in this work satisfies the condition that $Q \geq \pi/r$ and so the following approximate formula was used. The polydispersity of the number, *M*, in a stack is retained and the angle brackets in the equation (11) below indicate an average over a distribution of *M* with standard deviation σ_M.

$$I_M(Q) \approx \frac{N_P\Delta\rho^2A h^2 2\pi}{Q^2}\,\frac{I_B(Q\cos\theta)+\left\langle I_C(Q\cos\theta)\right\rangle_M}{h^2} \qquad (11)$$

Comparison of lines (b) and (d) in figure 5 give an indication of the quality of this "large disc" approximation. It is excellent except that the troughs between the peaks are slightly underestimated and, as expected, it breaks down at low Q.

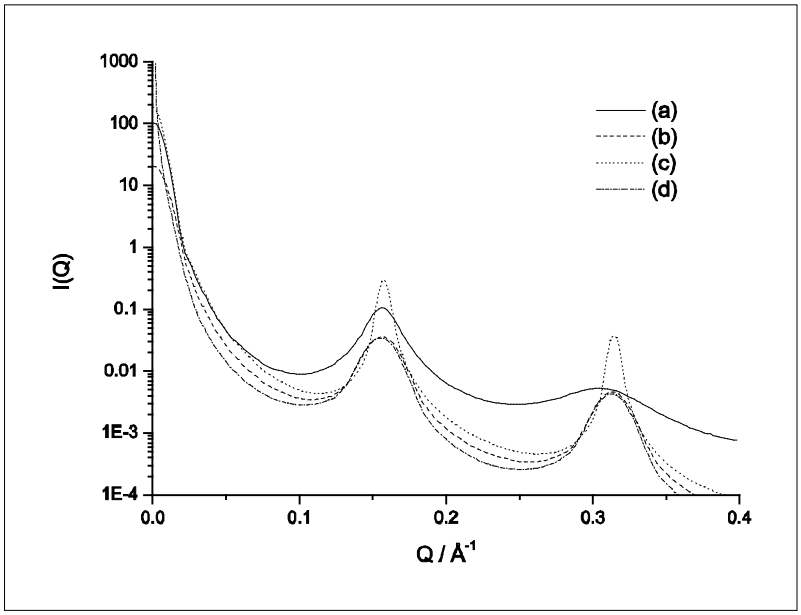

Figure 5. Scattering intensity expected from (a) the Hosemann model with a fluctuating gap between the plates and the regular but finite stack with (b) 4 ± 2 plates and (c) 12 ± 6 plates in the stack. For (a) to (c), the plate radius is 200Å with a polydispersity of 40% and a plate thickness of 10Å. For (d), the stacking is the same as for (b) but it is calculated in the large disc approximation.

It is useful to evaluate equation 10 for some typical parameter values in order to guide our interpretation of the scattering data. First we consider the interpretation of the widths of the pseudo Bragg peaks. Figure 5(a) shows the scattering calculated for a stack of 10±2 discs of identical thickness (h = 10 Å, $\sigma_h = 0$) separated by a soft phase layer of mean thickness s = 30 Å and standard deviation, $\sigma_s = 5$ Å. It shows peaks at $Q = n(2\pi/(h+s)) = n \cdot 0.157$ Å^{-1} as expected from a structure with a period of 40 Å. It illustrates that the width of the pseudo Bragg peaks increases with their order as is expected for this type of disorder. Inspection of the experimental data (see for example figures 8 to 11) indicates that the first and second order peaks are of nearly the same width so variability in the soft (or hard) layers' spacing is not the primary cause of the large peak width. The other possible source of broadening is the finite number of discs in the stack. Figure 5(b) also shows the scattering calculated for a stack of 4±2 discs of identical thickness (h=10 Å, $\sigma_h = 0$) separated by a soft phase layer of identical thickness (i.e. s = 30 Å, $\sigma_s = 0$). It can be seen that the peaks have the same widths and so this suggests that the origin of the peak widths in the experimental data is the small number of discs in a stack. Figure 5(c) shows the scattering calculated for a stack of 12±2 discs of identical thickness (h = 10 Å, $\sigma_h = 0$) separated by a soft phase layer of identical thickness (i.e. s = 30 Å, $\sigma_s = 0$) which has narrower peaks illustrating that the peak width is inversely proportional to the number in the stack irrespective of the details of the model. More precisely the full width at half maximum of the pseudo Bragg peaks, ΔQ, is given by $\Delta Q \sim M\, Q_{001}$, where Q_{001} is the position of the first order peak. This is essentially a description of a finite, one-dimensional crystal and the scattering may be formulated more simply using formulae analogous to a diffraction grating with M slits:

$$I_M(Q) \approx \frac{N_P \Delta \rho^2 A h^2 2\pi}{Q^2} \left(\frac{\sin Qh/2}{Qh/2} \right)^2 \left\langle \left(\frac{\sin MQd/2}{\sin Qd/2} \right)^2 \right\rangle_M \qquad (12)$$

where $d = h + s$ is the total thickness of a hard and a soft layer and the angle brackets indicate an average over a distribution of M with standard deviation, σ_M.

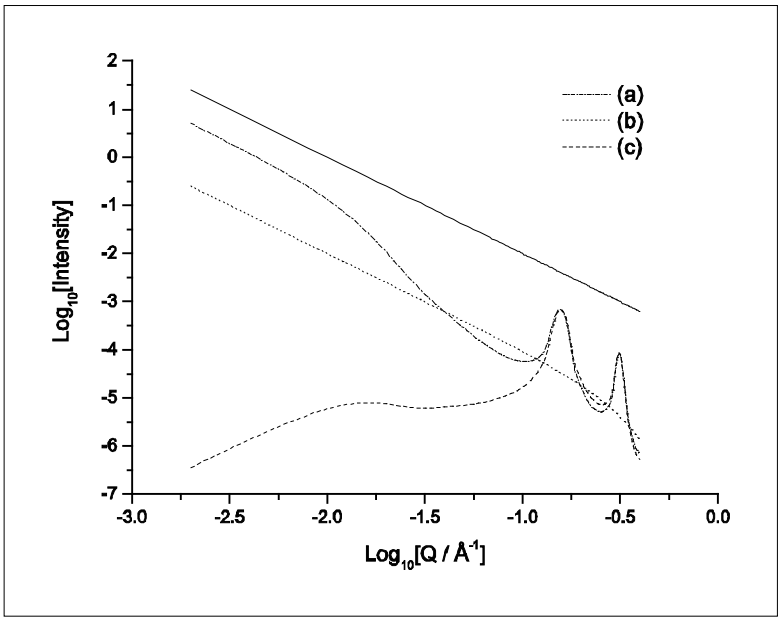

Figure 6. Showing intensity expected from (a) stacks of four discs, (b) single discs and (c) stacks of four with the mean electron density of the stack matched to the surroundings. A line of slope=-2 is shown for comparison.

For a single thin disc the scattering for $2\pi/h \geq Q \geq \pi/r$ follows a Q^{-2} power law decay. Figure 6 shows the scattering expected from single discs (from equation 10 with M=1) and stacks of four discs (from equation 10 with M=4) as a log-log plot. It demonstrates that the initial Q^{-2} power law decay is characteristic of both single and stacked discs, provided the overall shape remains highly anisotropic. However, the stacked disks show a greater intensity near Q = 0 and there is a region where the scattering from the stack falls more rapidly than as Q^{-2}. The absence of such a feature in the scattering would suggest that a sample comprised predominantly single delaminated discs. However, some of our scattering data show pseudo Bragg peaks, suggesting stacked discs but no such extra increase in the scattering at $Q \sim 0$. This leads us to consider other structural features that might suppress the intensity at $Q \sim 0$. The height of the maxima described by the finite one dimensional crystal $\left(\frac{\sin MQd/2}{\sin Qd/2} \right)^2$ term in equation 12 are the same. However, the physical origins of the peaks are different. The zero order peak (at Q~0) results from the contrast between the crystal and its surroundings and is similar to the "crystal" term in the Hosemann formulation. The higher order peaks are pseudo Bragg peaks resulting from the internal periodic structure of the crystal and arise from "Babinet" terms in the Hosemann formulation. If the crystal were surrounded by material whose electron density was the same as its average electron density, the zero order peak would have zero intensity. In order to describe the scattering from stacks of plates that are

embedded in a larger aggregate of similar composition, a second term has been included so that the contrast between a crystal and its surroundings can be adjusted.

$$I_M(Q) \approx \frac{N_P \Delta\rho^2 A h^2 2\pi}{Q^2}\left(\frac{\sin Qh/2}{Qh/2}\right)^2 \left\langle \sin^2 MQd/2 \right\rangle_M \left(\frac{1}{\sin\ Qd/2} - \frac{2\beta}{Qd}\right)^2 \quad (13)$$

In this equation, β is used to adjust the electron density of the surroundings of any particular stack of plates. If the mean electron density of a stack relative to the pure solvent is $\Delta\bar{\rho} = \Delta\rho\, h/(h+s)$, then the above formula assumes that the mean scattering electron density relative to pure solvent of the surroundings of the stack is $\beta\Delta\bar{\rho}$ as illustrated in figure 7. In a very dilute suspension $\beta = 0$ is expected and the zero order peak would have its full intensity. In an aggregate of many crystals at random orientations, $\beta = 1$ is expected and the zero order peak would have zero intensity. Figure 6(a) and 6(c) shows two extremes with $\beta = 0$ and $\beta = 1$, respectively.

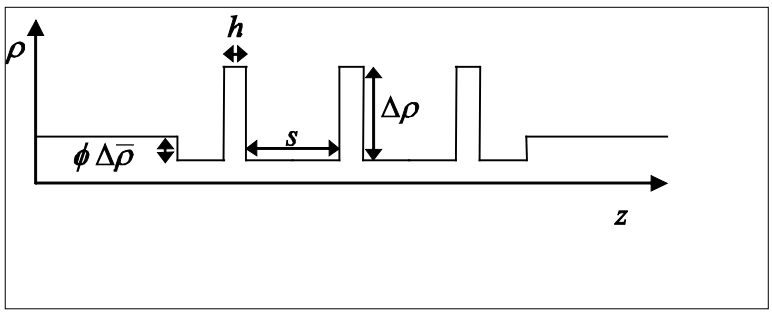

Figure 7. Schematic diagram of electon density as a function of distance, *z*, perpendicular to the plane of a stack of three plates.

In general, it is possible that a suspension of clay may contain two types of particle: single delaminated discs and stacks of discs. The surroundings of the two types of particle might also be different, with the possibilities ranging from pure solvent to similar particles as described above. In this case, the scattered intensity is given by the weighted sum of the scattering from stacks and scattering from single discs.

$$I(Q) \approx \frac{\Delta\rho^2 A h^2 2\pi}{Q^2}\left(\frac{\sin Qh/2}{Qh/2}\right)\times$$
$$\left(N_M \left\langle \sin^2 MQd/2 \right\rangle_M \left(\frac{1}{\sin\ Qd/2} - \frac{2\beta_M}{Qd}\right)^2 + N_1 \sin^2 Qd/2 \left(\frac{1}{\sin\ Qd/2} - \frac{2\beta_1}{Qd}\right)^2\right) \quad (14)$$

where the subscripts *M* and 1 refer to the stacks of *M* discs and the single delaminated discs respectively. For fitting the scattering data in this work, we have assumed that $\beta_M = \beta_1$ and combined the plate volume, contrast and incident intensity into a single scaling factor, *S*.

$$I(Q) \approx \frac{S}{Q^2}\left(\frac{\sin Qh/2}{Qh/2}\right)\left((1-x)\left(\left\langle \sin^2 MQd/2 \right\rangle_M + x \sin^2 Qd/2\right)\left(\frac{1}{\sin\ Qd/2} - \frac{2\beta}{Qd}\right)^2\right) \quad (15)$$

where *x* is the fraction of the particles that are single discs rather than stacks.

The scattering from the suspensions of clay has been analysed using Eq. 15. The seven model parameters $S, h, d, M, \bullet_M$, j and x have been adjusted by least squares fitting to fit the shape of the data. Initial values were estimated as follows. For scattering data with a Q^{-2} behaviour at low Q, it was expected that x~1. The value of the repeat distance, d, was estimated from $d \sim 2\pi / Q_{001}$ where Q_{001} is the position of the first order pseudo Bragg peak. The number of plates in the stacks was estimated using $M \approx \Delta Q / Q_{001}$ where ΔQ is the full width at half maximum of the first order peak. The plate thickness was taken at 10Å in accordance with the known structure of the clays [van Olphen 1977 and Rockwood Additives 2003].

Results

1. Claytone suspensions

As expected, the scattering from dry Claytone powder is most intense. With a high particle concentration and a high electron density difference between clay and air the intensity is at least two orders of magnitudes larger than that for the suspensions.

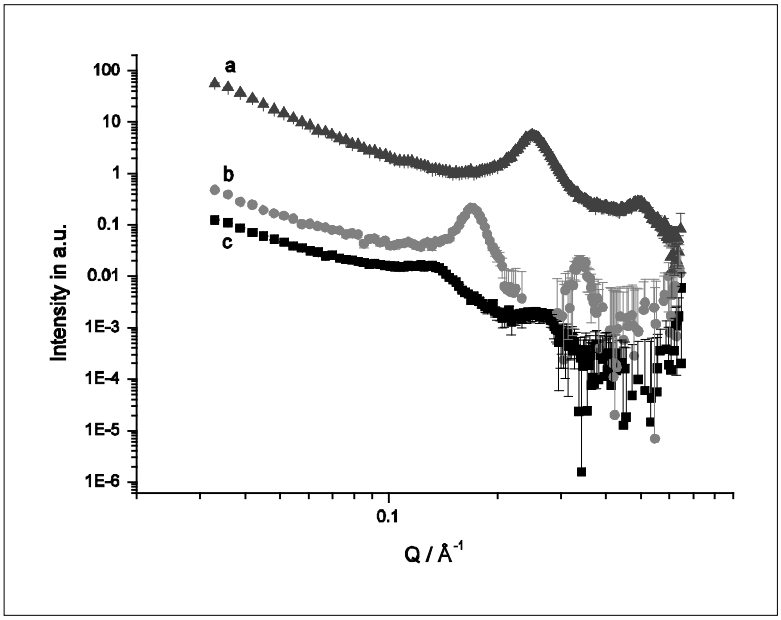

Figure 8: Scattering data from a) Claytone dry powder, b) 1% suspension of Claytone in K15 multiplied by 10 and c) 1% suspension in toluene.

The peak from dry Claytone powder implies a repeat distance of 25 Å which is consistent with 10 Å thick discs [Van Olphen 1977] with surfactant layers of about 15 Å thickness. Comparison of scattering data from Claytone AF powder with dispersions in K15 and toluene shows that the pseudo Bragg peaks are not caused by non-dispersed powder. On forming a suspension we observe a clear increase in the repeat distance of the plates from 25 Å in the powder to 36 Å in K15 and 46 Å in toluene. Assuming a plate thickness of 10 Å, this indicates that the gap between the plate surfaces has increased from 15 Å to 26 Å in K15 and 36 Å in toluene. This suggests that the aggregates in the powder are delaminated by the solvents but subsequently self assemble into ordered stacks within the dispersion. This effect is

most prominent in K15 but there is also some evidence of stacking in toluene dispersions.

Comparing the suspension in toluene with the suspension in K15 we find that the peak from the toluene suspension has shifted to lower Q. It is broader and less prominent. This indicates that the clay is well delaminated and the stacks forming within the dispersion have fewer sheets. A gap of 36Å suggests that the surfactant stabiliser chains are nearly extended (extended length ~22Å, rough estimate for the surfactant mixture). This suggests that the gap contains both surfactant and toluene which swells the surfactant. Powder and toluene data agree well with literature values of, respectively, 24.3 Å and 46.5 Å. [Ho 2001]

The K15 molecules have a length of about 17 Å when extended and they have a strong tendency to associate into antiparallel dimers (length 24 Å) in the bulk [Leadbetter et al 1975]. From the size of the gap we infer that the aggregate is formed by a single layer of K15 molecules intermixing with two extended chains of the steric stabiliser.

The narrower peaks indicate that the nematic liquid crystal matrix promotes larger stacks than toluene. This may result from the interaction of the K15 molecules with the surfactant on adjacent plates which would tend to "hold" the plates together.

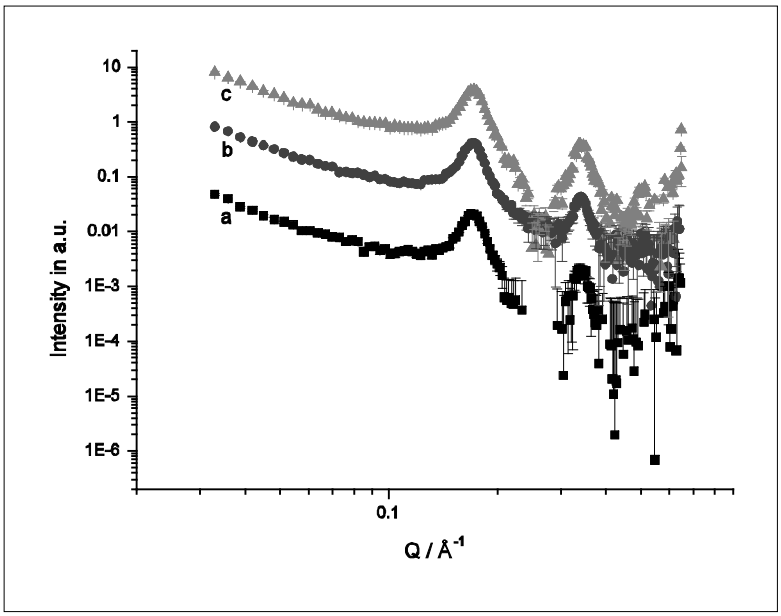

Figure 9: Temperature scan of 1% Claytone AF in K15. Time elapsed between the first measurement (25° C Heating) and the last (25° C Cooling): 15 h. The curves were shifted for clarity. a) 25°C heating, b) 40°C times 10 , c) 25°C cooling times 100.

When the liquid crystal is heated from the nematic into the isotropic phase no observable change in the peak position takes place (see Figure 9). This implies that the bonding between the plates that is, to some extent, mediated by the K15, is independent of the state of bulk K15 surrounding the plates. The inter-plate adhesion is so strong that it cannot be overcome by thermal agitation, even when the bulk is in the isotropic phase. The change in intensity between the first and last measurement can be understood in terms of the experimental schedule. At each temperature there

was a one hour wait time followed by a two hour data acquisition time. A temperature sequence of 25°C, 30°C, 35°C, 30°C and 25°C was run so that 15h elapsed between the first and the last measurement. Since the suspensions are only stable up to ~24 h and aggregates at the bottom of the vial were generally observed after 15h, it is clear that some change of the numbers of particles in the beam takes place. With shorter measurement times it would be possible to correlate floc formation with the scattering signal from the aggregating suspension. In a future paper we will report the results from these observations.

It seems that the monolayer of K15 molecules between the plates is a stable state as scattering from more dilute suspensions (Figure 10) does not show a shift in the peak position to lower Q.

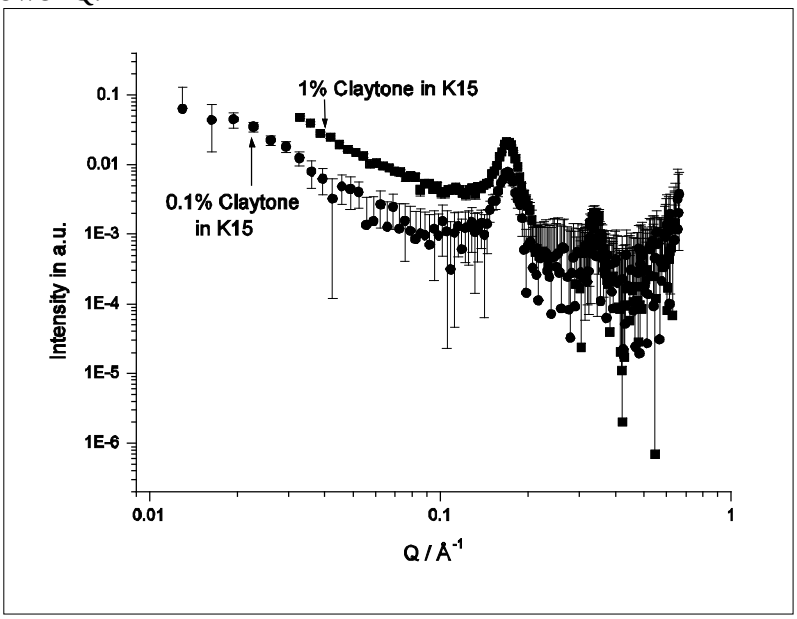

Figure 10: Scattering from 0.1% and 1% Claytone in K15.

In figure 10 the signal from the clay is very weak in the 0.1% curve and noisy compared to the 1% curve. However the first order peak is still in the same position. This implies that the number of stacks has decreased but the spacing between the plates in the stack has not changed.

To show that our theoretical model describes our experimental system, we have fitted the scattering data from Claytone and Laponite suspensions in two different host solvents using equation 15. This fitting allows us to confirm our model and to determine values for the stack height and plate spacing from the data.

As there are no discernible differences in the peak position between the scattering from the suspension of different concentrations and temperatures, we consider only the case of 1% w.w. clay at 25°C for fitting purposes.

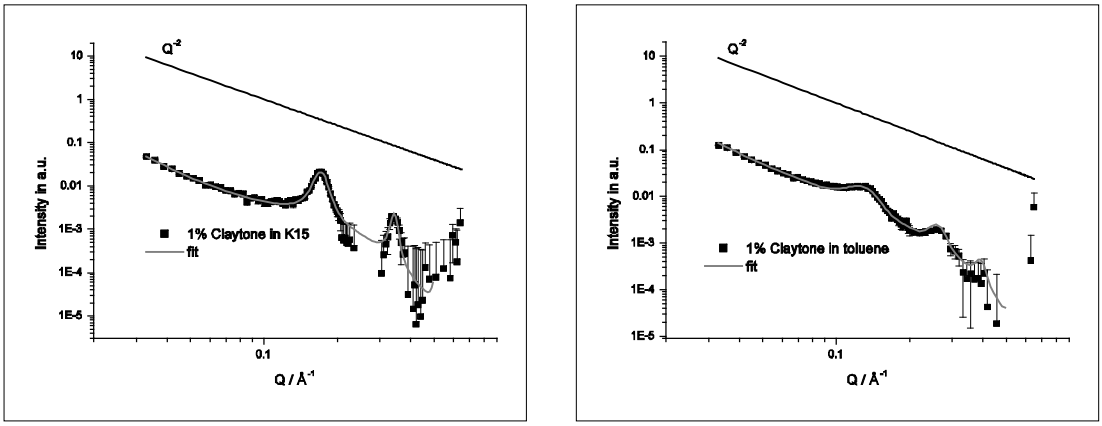

a b

Figure 11. a) 1% Claytone in K15, data and fit. b) 1% Claytone in toluene, data and fit. A line of slope –2 is included for comparison.

Figure 11 shows clearly that at low Q, i.e. Q< 0.1 $Å^{-1}$, the scattering data follows a Q^{-2} power law decay characteristic of both single and stacked discs. However there is no step with a greater exponent than 2 as shown in figure 6. Since the pseudo Bragg peaks indicate the presence of stacks, this suggest that the mean electron density of the stacks is matched by the surrounding. The pseudo Bragg peaks in the region 0.1 <Q< 0.4 $Å^{-1}$ are fitted assuming a combination of free "large" single discs and free stacks of "large" discs (equation 15). The model is in reasonable agreement with the data. However, it is not completely satisfactory for the K15 suspensions. The observed scattering at Q ~ 0.25$Å^{-1}$ is negative and hence not shown in the graph. Since this is the region where the nematic peak occurs, it is possible that this peak has been reduced by the presence of the clay plates. Background subtraction of pure K15 overcompensates using equation 1 for the peak and leads to an unrealistically low intensity in that region.

We start the fitting procedure by assuming a fixed plate thickness of 10 Å and a periodicity of 35 Å (K15 suspensions) and 45 Å (toluene suspension) calculated from the first order peak positions. The thickness of the clay plates is fixed, since the model is not very sensitive to variation in the thickness of the hard phase. The value of 10Å has been confirmed in the literature [Cione *et al* 1998].The number of plates is estimated by the full half-width of the first maximum in the scattering data divided by the first order peak position. These parameters are allowed to vary and the best fit is found by least squares fitting to the data. The proportion of single plates relative to the stacks in the system is a parameter which changes the height of the peaks relative to the Q^{-2} decay line. As mentioned earlier, the model described by equation 15 assumes that the standard deviation on the soft phase and hard phase are zero since the peak width is the same for the first and second order peaks. Including standard deviations on the soft phase or hard phase would make the second order peak relatively broad and diminish its height.

The best fits for the scattering data are shown in Figure 11 and the parameter values for these fits are given in Table 1. The dimer length of K15 is 24 Å and so an interplate separation of 26 Å is consistent with the model of two extended surfactant chains interlocking with a single layer of K15 dimers. The ordering influence of K15

is most visible in the percentage of single clay plates in the suspension. Only 28% of the clay present in suspension is in the form of free individual particles. The rest exist in stacks of about 5±2 plates.

In the case of the toluene suspensions, the situation is quite different. There are fewer plates in the stacks, 2 compared to 5, the gap between the plates has increased from 27Å to 38Å and most of the particles in suspension (67%) are free single plates indicating less overall order imposed on the system. This demonstrates clearly the influence of the solvent molecular structure on the nature of the dispersion.

Parameter	1% Claytone in K15	1% Claytone in toluene
Plate thickness, h	10 Å	10 Å
Periodicity, $h+s$	37Å	48 Å
Soft phase thickness, s	27 Å	38 Å
No. of plates in stack, M	5	2
Standard deviation of no. of plates, σ_M	2	1
Percentage of single plates in suspension $\frac{x}{x+(1-x)M}*100$	28%	67%
Volume fraction of stacks in solvent surrounding a given stack , j	0.3	0

Table 1. Fit parameters for all fits shown for Claytone.

The average number of plates in a stack, M, in its standard deviation, σ_M, are correlated. The fit changes very little when M or σ_M vary as long as their sum stays constant.

2. Laponite suspensions

In this case the particles used have approximately the same thickness as the Claytone plates, however they are much smaller in diameter. This difference in diameter also gives rise to a different structural behaviour; the Laponite plates may be considered to be rigid. The steric stabiliser on the surface of the Claytone does not greatly alter the aspect ratio, however using the same stabiliser on Laponite changes the overall shape of the particle. The aspect ratio decreases from 1:26 (untreated) to 1:8 (surface treated). This means that the particle is now effectively more like an ellipsoid and less like a disc.

Despite the fact that the particles are smaller, they have a greater tendency to aggregate than the Claytone plates. This can be observed when the suspension is placed in a thin cell (a 2mm diameter capillary or between microscope slides). Large open flocs start to form in less than 1 hour with complete phase separation occurring after 24 hours. Claytone suspensions also sediment and phase separate after 24-36 hours, but do not form these large open flocs.

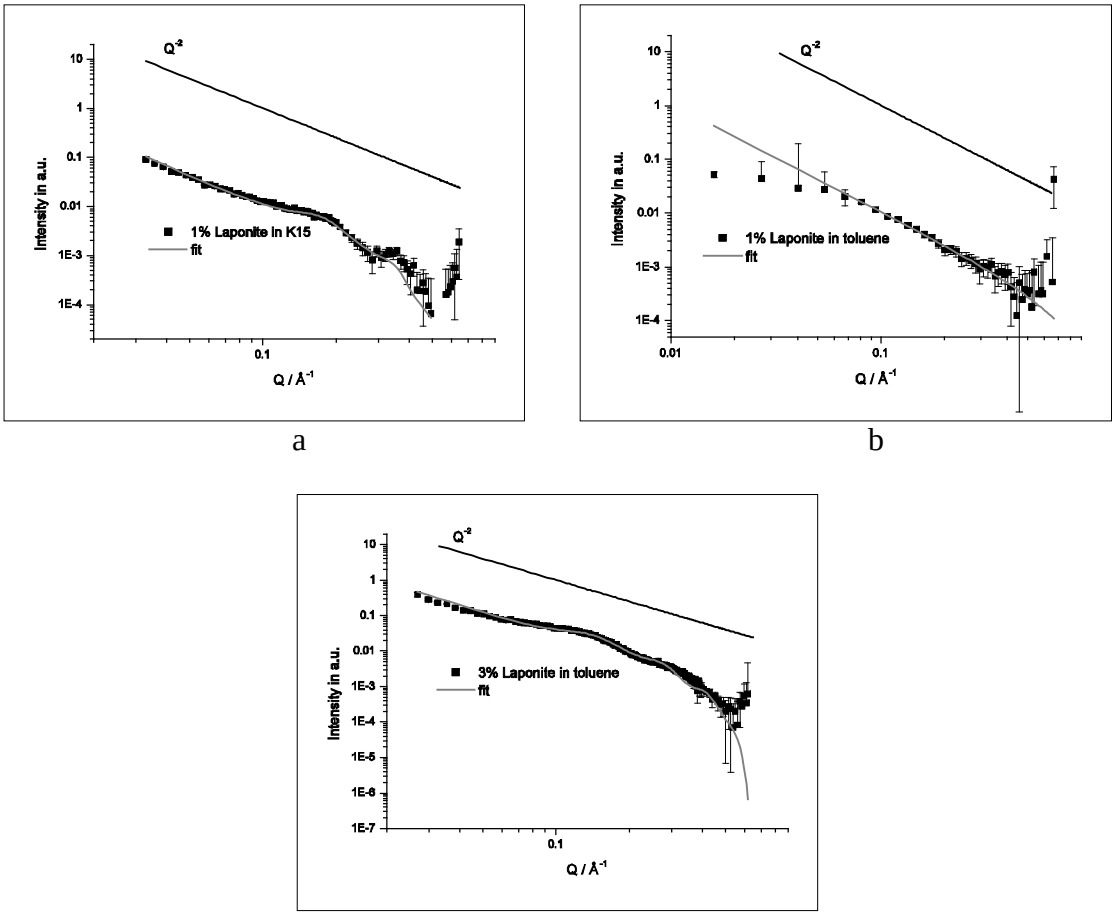

Figure 12. Laponite suspensions. a) 1% Laponite in K15, data and fit. b) 1% Laponite in toluene, data and fit. c) 3% Laponite in toluene, data and fit. A line of slope –2 is included for comparison.

As in the Claytone suspensions, the scattering data from Laponite suspensions does not change with variation in temperature (from 25°C to 40°C) or concentration (from 0.1% w./w. to 5% w./w). The pseudo Bragg peaks that are so prominent in the data for Claytone suspensions become much weaker, they almost disappear, for Laponite suspensions giving featureless scattering data that are difficult to fit.

The data for K15 as solvent cannot be fitted by consideration of single plates only as might be assumed from the absence of prominent peaks. Nevertheless, 77% of the plates are free delaminated discs and the stacks consist of 2±1 plates only, i.e. the stacking tendency is minimal.
Toluene delaminates the clay completely in the 1% suspension and its scattering can be fitted by single plates alone. For the 3% suspension we can fit the data by assuming the same periodicity as for Claytone but the stack size is 1±1 plates, that is we have again a completely delaminated clay with the occasion pair of plates.

Parameter	1% Laponite in K15	1% Laponite in toluene	3% Laponite in toluene
Plate thickness, h	10 Å	10 Å	10 Å
Periodicity, $h+s$	36 Å	-	45 Å
Soft phase thickness, s	26 Å	-	35 Å
No. of plates in stack, M	2	-	2
Standard deviation of no. of plates, σ_M	1	-	1
Percentage of single plates in suspension $\frac{x}{x+(1-x)M}*100$	~90%	100%	~90%
Volume fraction of stacks in solvent surrounding a given stack , j	0.27	0	0.15

Table 2. Fit parameters for all fits shown for Laponite.

The fitting values show that the Laponite behaves very differently from the Claytone. We know that in K15 open flocs are formed quite quickly, certainly within our measurement time (2 hours) as this may be observed by optical inspection of the capillaries. Nevertheless the fitting parameters, maximal 2 plates in a stack and 90% free discs, indicate that the flocculation does not involve an enhanced stacking. The flocs are probably aggregates of plates with random orientations.

Conclusions

The clay suspensions in K15 are not stable over long periods of time. This is probably due to limited compatibility between the surfactant stabiliser and the liquid crystalline host. The suspensions in toluene are stable and provide a useful comparison. Further work will focus on refining this system to achieve better stabilisation of the particles in the liquid crystalline medium to give longer term stability.

Nevertheless, the suspensions are sufficiently stable for analysis to give insight into the behaviour of anisometric particles in an anisotropic host. Particles with a greater aspect ratio, in this case Claytone, have shown a strong tendency to self organise into stacks, this effect is most prominent in the case of the liquid crystal suspensions where 72% of all particles present are stacks with ~5 sheets. This effect may also be observed in the toluene suspensions, but to a much lesser extent with only 33% of all particles being stacks. The increased tendency of K15 to form stacks as compared to the small molecule solvent toluene suggest that the larger K15 molecules enhance the interaction between the plates. Since the effect was observed above and below the clearing temperature it does not appear to be a result of the interaction with the surrounding matrix. Stack formation is a frequently observed phenomenon in suspensions where montmorillonite is the suspended particle. Determination of the number of stacks in a suspension has not previously been attempted but the numbers of plates in a stack in isotropic dispersing media are similar to our results. Numbers

given in the literature vary with solvent and surface treatment from 1 [Ho et al 2001], 3 [Shang et al 2002] up to 6 [Hanley and Muzny 2003]. For K15 solvent, gap between the plates in a stack, 26-27 Å, appears to be independent of temperature, concentration and size of dispersed platelets. This merits further investigation. Small angle neutron scattering could give us detailed information about the arrangement of molecules at and around the plate surface because contrast variation may be used.
Laponite, chemically similar to Claytone but with a much smaller aspect ratio, lacks the strong tendency to form stacks. The 1% toluene solution showed no pseudo Bragg peaks suggesting that the clay was completely delaminated. In order to detect any stack formation in toluene at all we have fitted data from 3% suspensions where pseudo Bragg peaks just emerge and indicate the same spacing of 35Å similar to the spacing for Claytone in toluene. Even in K15 we find only pairs of plates, again with the same spacing as for Claytone, and only 23% of the particles are these stacks. Even after floculation, at the end of our runs, the peaks have neither shifted nor increased in intensity indicating that the flocs are aggregates of randomly oriented plates.

Acknowledgements

We would like to thank Steve Bodley for his assistance performing SEM measurements. One of the authors (CP) would like to acknowledge the financial support of the EPSRC and Hewlett-Packard as part of the IMPACT Faraday Partnership.

References

Bateman, J.E. *et al*, 1987, Nucl. Inst. and Meth. In *Phys. Res.,* **A259**, 506-520.
Balnois, E. *et al*, 2003, *Langmuir*,**19,** 6633-6637
Cione *et al*, 1998, *J. Coll. Int. Sci*. **198**, 106-112.
Hanley, H.J.M. and Muzny,C.D., 2003, *Langmiur*,**19,** 5575-5580
Ho, D.L. *et al*, 2001, *Chem. Mater.*,**13,** 1923-1931
Hosemann, R. and Bagchi, S. N., 1962, *Direct Analysis of Diffraction by Matter*, Amsterdam (North Holland Publishing Co.)
Huang, T.C. *et al*, 1993, *J. Appl. Cryst.*, **26**, 180-184.
Jordan, J.W., 1949, *Journal of Physical & Colloid Chemistry*, **53,** 294-306
Kawasumi, M. *et al*, 1999, *Applied Clay Science*, **15**, 93-108
Kawasumi, M. *et al*, 1996, *Mol Cryst. Liq. Cryst.*, **281**, 91-103
Kratky and Porod, 1948, *Act. Phys. Austr.*, **2**, 133.
Kreuzer M. and Eidenschink, R., 1996, "Filled Nematics" in *Liquid Crystals in Complex Geometries*, Ed. G.P. Crawford (Taylor and Francis).
Leadbetter, A.J., Richardson, R.M., Colling, 1975, *J. de Physique (Paris)*, **36**, C1,37-43
Lin *et al* , 1987, *J Phys Chem* , **91**(2),406-13
Rockwood Additives Product Information, 2003.
BDH Product Information, 1986.
Shang, C. *et al.*, 2002, *Soil Sci.Soc.Am.J.*, **66,** 1225-1230
Stark, H., 2001,*Physics Reports*, **351**, 387-474
Van Olphen, H., 1977, *An Introduction to Clay Colloid Chemistry* 2nd Ed., New York (John Wiley & Sons).
Zhivkov, A.M., Stoylov, S.P.,2003, *Colloids and Surfaces A*, **209,** 315-318